Two-Dimensional NMR Characterization of the Deoxymyoglobin Heme Pocket†

Scott C. Busse and Thomas Jue*

Department of Biological Chemistry, University of California—Davis, Davis, California 95616-8635

Received January 5, 1994; Revised Manuscript Received June 30, 1994®

ABSTRACT: Traditionally, assigning the heme protein resonances has relied heavily on the comparison of spectra arising from protein reconstituted with specifically deuterated hemes and the native form. Such an approach can identify tentatively the broad, overlapping signals in the Fe(II) high-spin heme protein spectra. Although 2D NMR studies have reported alternative approaches to detect and assign paramagnetic signals, their effectiveness is limited primarily to Fe(III) low-spin systems and still depends upon isotopic labeling results to be definitive. For deoxymyoglobin, the reported 2D techniques have not produced any spin correlation maps. Nevertheless, our study demonstrates that the deoxymyoglobin spin correlations are indeed detectable and that a complete heme assignment, except for the meso protons, is achievable with only 2D NMR and saturation-transfer techniques. The 2D maps improve the spectral resolution dramatically and permit a comprehensive analysis of the deoxymyoglobin signals' temperature dependence, which supports the hypothesis that the electronic orbital ground state has contributions from both ^5E and $^5B_2$. The results also indicate a structural perturbation in the vicinity of the 2 vinyl group as the protein undergoes the transition from oxy- to deoxymyoglobin state and a significant contribution from zero field splitting. Moreover, saturation-transfer experiments show that NMR can observe directly oxygen binding kinetics.

Although many studies have detailed the myoglobin structure in various ligation and oxidation states (Antonini & Brunori, 1971; La Mar, 1979; Takano, 1977a,b; Phillips, 1980; Ho & Russu, 1981; Mabbut & Wright, 1985; Dalvit & Wright, 1987), questions still persist about the specific interactions that regulate oxygen binding. A key issue centers on the electronic and solution structure of the Fe(II) deoxymyoglobin, which along with oxymyoglobin forms the physiologically relevant state. Unlike the Fe(III) myoglobin states, Fe(II) deoxymyoglobin has resisted a thorough NMR analysis (Emerson et al., 1990). Its broad, overlapping signals, resonating near the diamagnetic region, pose formidable spectroscopic challenges. 2D[1] NMR methodology has failed so far to produce a complete definitive map. Consequently the resonance assignment strategy has relied almost exclusively on ^1H, ^{13}C, and ^2H studies of mutant myoglobin or myoglobin reconstituted with isotopically labeled hemes (Sankar et al., 1987; La Mar et al., 1993). Bootstrapping from the isotopic labeling data leads then to additional signal assignments (Yamamoto et al., 1992; Banci et al., 1993). However, the isotopic labeling strategy establishes a convincing identification of only a few distinguishable deoxymyoglobin resonances and entails time-consuming, but elegant, synthesis of specifically labeled hemes (Smith et al., 1986).

Still, the initial, critical step for protein structure analysis demands definitive resonance assignment. For heme proteins, the resonance assignment assumes an even greater importance, because it forms the basis to understand both the solution and the electronic structure. The hyperfine-shifted, paramagnetic signals, described by both the contact and the dipolar terms (Shulman et al., 1971; La Mar, 1979; Jesson, 1973), reflect the electronic structure and can, in particular, elucidate the orbital ground state (La Mar et al., 1993). As a result, structural perturbations that alter the electronic state are often manifested in the hyperfine chemical shift pattern, which points to the molecular mechanisms controlling oxygen binding affinity (La Mar, 1979). The specific relationship between the electronic structure and the protein structure in deoxy Mb, however, still remains unclear.

Assigning the deoxymyoglobin resonances also provides insight into another type of protein function, its actual function in the cell. Some debate still surrounds the role of cellular myoglobin: Is it merely for oxygen storage, as stated by the conventional view? Or does it have a role in facilitating oxygen transport (Wittenberg & Wittenberg, 1989)? Even though NMR studies have detected the myoglobin signals in myocytes (Kreutzer & Jue, 1991), the results indicate that the solution and tissue spectra of deoxymyoglobin may differ substantially, especially in the upfield region. In contrast to the solution spectra, no peaks in tissue appear around −2.8 ppm. It raises the question whether the cellular and solution myoglobin structures differ (Kreutzer et al., 1992). If a difference exists, then identifying the amino acid or heme group in deoxymyoglobin that gives rise to the signals near −2.8 ppm would also yield insight into myoglobin's protein structure and, perhaps, its physiological role in the cell.

We report herein that 2D techniques can assign, except for the meso protons, all of the heme ^1H resonances as well as those of some surrounding amino acid residues in deoxymyoglobin, independent of any isotopic labeling or mutant Mb experimental data. Our study establishes an alternative to the isotopic labeling approach to interrogate heme protein structure, indicates a structural perturbation in the interaction of the 2-vinyl group, and supports the hypothesis of different populated electronic states, derived from both ^5E and $^5B_2$. It also demonstrates that NMR can monitor directly the oxygen binding kinetics in deoxymyoglobin. The results then open different opportunities to explore the structural and electronic mechanisms that influence oxygen binding in myoglobin.

† The research was support by grants from NIH (GM44916), the American Heart Association (92-221A), and the UCD Hibbard Williams Fund.

® Abstract published in *Advance ACS Abstracts,* August 15, 1994.

[1] Abbreviations: TOCSY, total correlation spectroscopy; NOESY, nuclear Overhauser enhancement spectroscopy; 2D, two dimensional; 1D, one dimensional; TPPI, time-proportional phase incrementation; WALTZ, wide-band alternating-phase low-power technique for zero residue splitting; TRIS, tris(hydroxymethyl)aminomethane; EDTA, ethylenediaminetetraacetic acid.

0006-2960/94/0433-10934$04.50/0

MATERIALS AND METHODS

Sample Preparations. Horse heart myoglobin (Sigma), without further purification, was dissolved in a D_2O buffer (25 mM phosphate, pH 7.4) to make a 10 mM solution. Centrifugation removed any undissolved material. The sample was then transferred to a 5-mm NMR sample tube, sealed with a gas-tight septum. An evacuation–purge cycle, with a vacuum pump and nitrogen, degassed the sample and removed the excess oxygen. Two to three equivalents of sodium dithionite, dissolved in 0.1 mL of D_2O buffer and injected through the septum, removed the remaining oxygen and reduced the heme from Fe(III) to Fe(II).

For oxy Mb, a Sephadex G-25 molecular size separation step followed the initial dithionite reduction of met Mb in a D_2O buffer (1 mM EDTA and 5 mM TRIS, pH 8.4). Concentrating the sample in an ultrafiltration cell (Amicon) produced a final 10 mM oxy Mb solution. Injecting 0.5 equivalent of dithionite into a degassed, sealed tube of deoxy Mb sample then yielded the 50/50 mixture of oxy and deoxy Mb. Although the protein preparation procedure minimized the Mb autoxidation rate from Fe(II) to Fe(III), about 10% met Mb still appeared within 1 h, detectable from both the distinct optical and NMR signals (Antonini & Brunori, 1971).

NMR. NMR spectra were recorded with a General Electric (GE) Omega 300, a GE Omega 500, or a Bruker AMX 400 spectrometer. Variable-temperature studies of deoxymyoglobin on the GE Omega 300 required a 10-kHz spectral width, 32 scans, presaturating irradiation for water suppression, and 1-Hz exponential apodization. The HOD line was referenced to 4.76 ppm at 25 °C, which was calibrated against DSS. At different temperatures, the HOD reference line was adjusted to reflect its temperature dependence. The variable temperature control unit maintained and recorded accurately the sample temperature within ±0.5 °C.

2D TOCSY (Braunschweiler & Ernst, 1983) experiments on the Bruker AMX 400 spectrometer utilized previously reported pulse sequences (Rance, 1987; Rance & Cavanagh, 1990) and TPPI (Marion & Wuthrich, 1983) for phase-sensitive detection. The spectra required a 12-kHz spectral width, 256 experiments with 1K complex points, 640 or 960 scans, and a 300–400-ms repetition time. Sufficient pulse power permitted the isotropic mixing (WALTZ) pulse to spin-lock the entire deoxy Mb spectral window. Typical 90° pulses ranged from 10 to 14 μs; spin-lock time varied between 5 and 10 ms. The signal phase of the first row of the 2D data set confirmed the efficiency of the spin lock. A presaturating pulse reduced the residual water resonance. The NOESY (Jeener et al., 1979) experimental parameters parallel the TOCSY ones. However, the NOESY mixing times varied between 20 and 75 ms. A sine bell squared function, shifted by 45° in each dimension, filtered the acquisition data. Zero filling to a final size of 1K by 1K real points improved the digital resolution.

Selective T_1 and transient NOE measurements utilized a monochromatic irradiation. For T_1, a three-parameter analysis extracted the relaxation rate from the inversion recovery data. The nonselective T_1 experiments were similar, except for the initial nonselective inversion pulse. NOE experiments subtracted spectra with off-resonance and on-resonance irradiation.

The 1D and 2D saturation-transfer experiments on the 50/50 mixture of oxy/deoxy myoglobin were performed on a GE Omega 500 spectrometer operating at 500 MHz proton frequency. For the 1D saturation-transfer experiments, subtracting spectra from a selective 60-ms irradiation of the peak of interest and from an off-resonance irradiation yielded the final spectra. Decoupler spillage was negligible at 50 Hz from the irradiation point. The spectral parameters included 4K real points, a 500-ms repetition time, 1600 scans, and a 10-Hz exponential apodization.

RESULTS

Hyperfine-Shifted Signals. An analysis of the temperature dependence is critical in setting spectral acquisition parameters, interpreting the data, obtaining insight into the local protein structure interaction, and probing the electronic structure. Figure 1 clearly shows that certain peaks become resolved only within a specified temperature range. With only 1D spectra, some uncertainty arises about the accuracy of any temperature analysis. With 2D TOCSY maps the resolution improves significantly, and the analysis is more certain. The temperature-dependent plots are also important in establishing calibration curves to account for any shifts in the various cross-peak positions associated with the potentially differential sample heating in the TOCSY and NOESY sequences.

Figure 1 (left panel) shows a bank of 1D ^1H NMR signals from deoxy Mb at different temperatures. Many peaks exhibit a paramagnetic temperature dependence and are not resolvable with 1D spectra under different conditions. In the downfield region between 15 and 10 ppm, three prominent peaks, a, e, and h, appear, Figure 1A. At 5 °C, Figure 1E, the signals at 13 ppm coalesce. At 45 °C, Figure 1A, however, coresonating signals become distinguishable and reveal the peaks' composite nature. Broad resonances w–z also appear in the upfield region, –2 to –10 ppm. The most prominent ones at –7.3 and –4.5 ppm show specific spectral changes between 5 and 45 °C, confirming their composite nature.

In Figure 1 (right panel), peaks a–d and h show the Curie temperature relationship, which typifies many hyperfine interactions. TOCSY maps at various temperatures help resolve the ambiguity in determining the chemical shift. The temperature coefficients (ppm/$(1/T)$) and the diamagnetic chemical shifts extrapolated from the y intercepts (ppm) for peaks a, c, and e are respectively 4664 (0.34), 3101 (3.32), and 4054 (0.17), while for b and h they are 567 (12.35) and 1322 (6.71). Peaks d, f, and g show anti-Curie behavior (–765 (15.07), –2166 (19.37), and –1020 (14.31)). Upfield peaks u, v, w, y, and z also show temperature dependence (–4010 (10.75), –2411 (5.33), –2365 (4.56), –1711 (0.91), and –2418 (0.34)).

Spin Correlation. Identifying the different spin systems may appear to be straightforward and is an essential step in characterizing a protein. Even though several studies have presented techniques to obtain correlation maps of primarily low-spin heme proteins (Yu et al., 1990; Sadek et al., 1993), the reported methodology has so far failed to produce any deoxymyoglobin cross peaks, despite repeated attempts. However, the acquisition parameters presented in the Materials and Methods section do produce deoxymyoglobin TOCSY maps at various temperatures. A typical map collected at 45 °C is shown in Figure 2A. Although the prominent three-proton a and h signals at 14.81 and 10.78 ppm, respectively, show no cross peaks, the d signal at 12.98 ppm couples to a resonance at 9.05 ppm, cross peak [4]. A heme methyl assignment is consistent with the TOCSY results for peaks a and h, but not those for d. Peak b at 14.08 ppm shows connectivity to two signals at 6.74 [1] and 1.58 ppm [2]. The peak cluster (c, d, e, and f) centered at 13 ppm shows six connectivities: Peak c, a single-proton peak, couples to signals

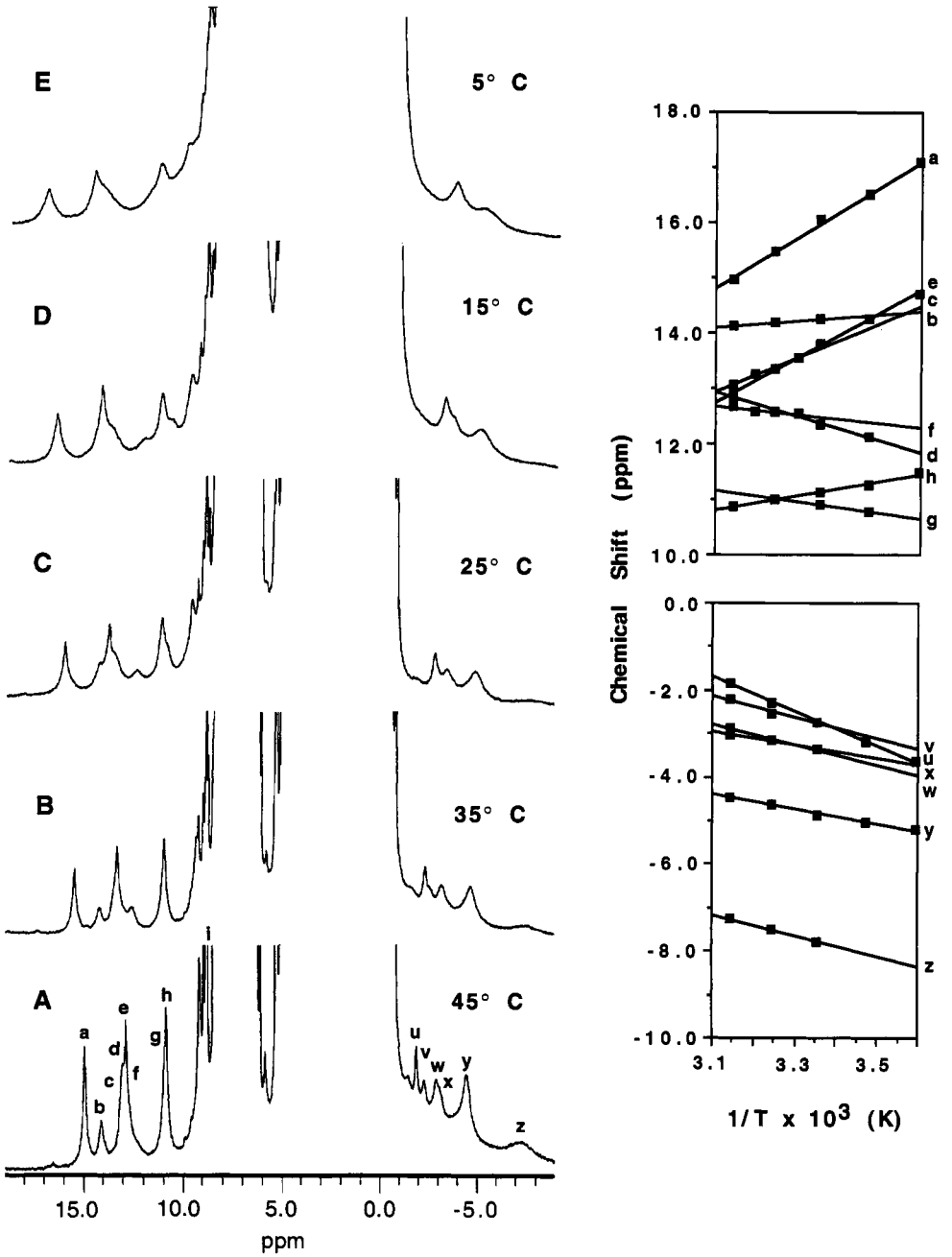

FIGURE 1: (Left panel) 300-MHz ^{1}H NMR spectra of 10 mM deoxymyoglobin in D_2O, 25 mM phosphate buffer, pH 7.4, at (A) 45 °C, (B) 35 °C, (C) 25 °C, (D) 15 °C, and (E) 5 °C. Resonances in the downfield and upfield regions are labeled with lowercase letters. (Right panel) Plot of the chemical shift versus reciprocal temperature (K) for the labeled resonances shown in the left panel.

at 5.10 ppm [5] and 2.01 ppm [7]; peak d, to a signal at 9.05 ppm [4]; peak e, to signals at 3.42 [6] and −1.84 ppm [8]. Peak f couples to signal g at 10.91 ppm [3], which in turn couples to two resonances at 6.44 [9] and 4.26 ppm [10]. In the upfield region peaks v and w at −2.25 and −2.87 ppm belong to the same spin system and couple to each other as well as to a resonance at 2.52 ppm [11,12]; peak u couples to signals at 12.65 ppm [8]. TOCSY maps at different temperatures also show distinct cross-peaks and support the cross peak connectivities outlined above. The TOCSY results recorded at 45 °C are tabulated in Table 1.

NOE Correlation. The TOCSY experiments have identified the various spin systems and have established a critical basis to map the intermolecular interactions. Figure 2B shows the corresponding 2D NOESY map of deoxy Mb at 45 °C. In the downfield region peak a connects to six signals. Two prominent ones are at 14.08 [16] and 1.58 ppm [18]. Peak c shows an interaction with several intramolecular nuclei, detected in the TOCSY map, and exhibits a common NOESY cross peak to h [14]. The composite peak (d, e, f) shows numerous intramolecular cross peaks [1, 2, 3, 4, 5, 6, 8, 14]. Peak g shows a connectivity to a peak at 4.26 ppm [10], which in turns exhibits an NOE cross peak to a resonance at 7.30 ppm. The amino acid residue corresponding to peak h also interacts with numerous other protons, as reflected in the many NOESY cross peaks. A prominent one connects h to a peak at 9.05 ppm [17]. Upfield, y shows an NOE to a resonance at 0.15 ppm, observed at lower contour levels. 1D transient NOE data also correlate the proximal histidyl NH signal at 74 ppm at 45 °C with signals at 13.03 and 8.66 ppm, data not shown. NOESY maps at different temperatures also strongly support the cross-peak connectivities observed at 45 °C. The NOESY data collected at 45 °C are also tabulated in Table 1. The summary of the heme cross peaks is listed in Table 2.

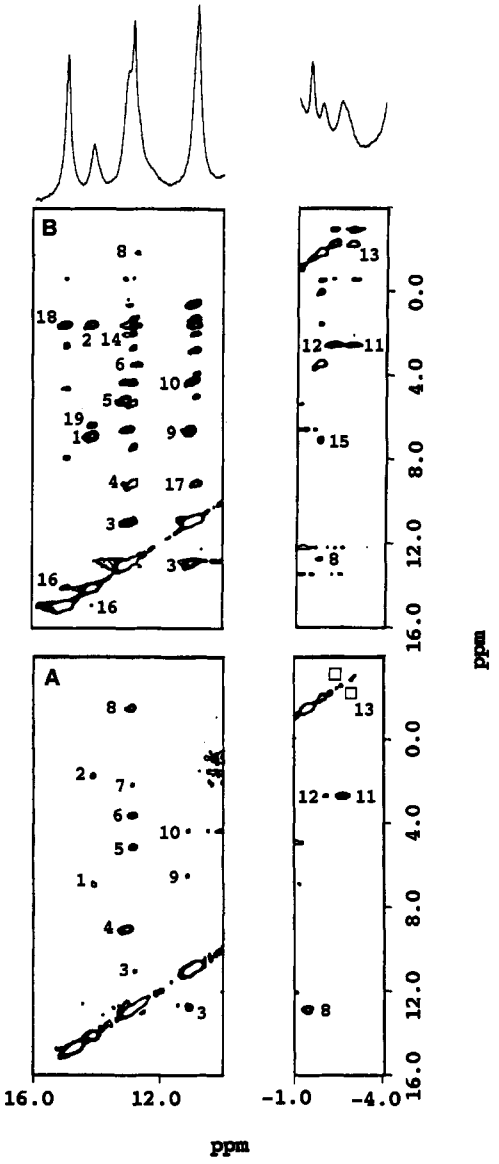

FIGURE 2: (A) Downfield and upfield portions of the 400-MHz 2D TOCSY NMR spectrum of deoxymyoglobin in D_2O and 25 mM phosphate buffer, pH 7.4, at 45 °C, collected with an 8-ms isotropic mixing time. Heme substituent and amino acid cross peaks are numbered. (B) Downfield and upfield portions of the 400-MHz 2D NOESY NMR spectrum of deoxymyoglobin collected under conditions similar to those for TOCSY but with a mixing time of 50 ms. The NOESY cross peak numbering is consistent with the TOCSY map.

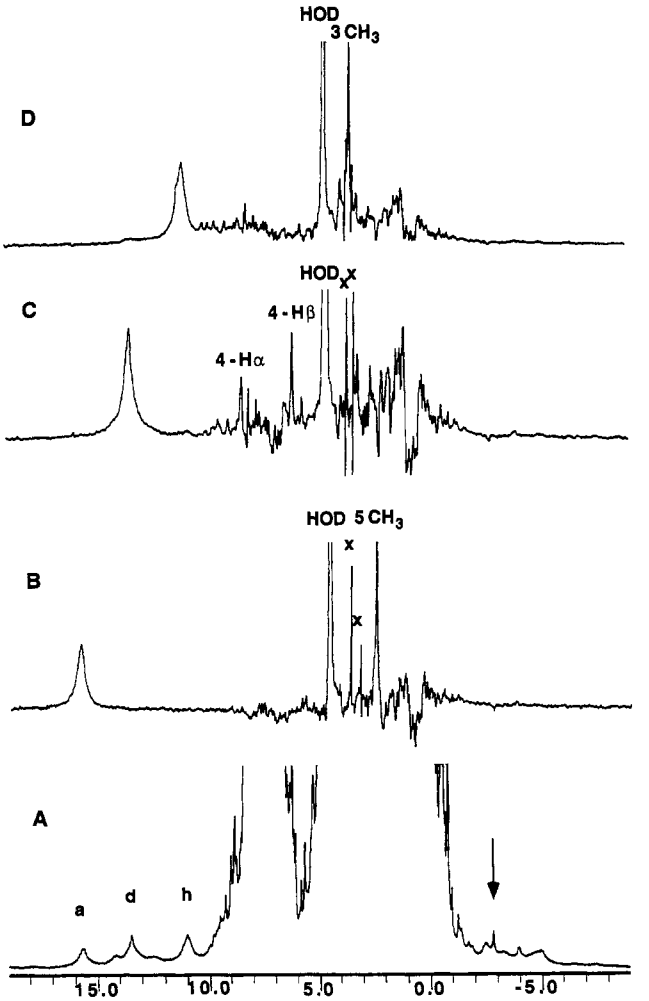

FIGURE 3: (A) 500-MHz ^1H NMR reference trace of a mixture of oxy- and deoxymyoglobin in D_2O, 1 mM EDTA, and 5 mM Tris, pH 8.7, at 30 °C. Saturating resonances a, d, and h yielded the 1D NOE difference spectra shown in panels B–D. The arrow identifies the resonance from the Val 68 residue γCH_3 in oxymyoglobin. (B) 1D NOE difference spectrum obtained by saturating resonance a. (C) 1D NOE difference spectrum obtained by saturating resonance d. (D) 1D NOE difference spectrum obtained by saturating resonance h. The two x signals arise from Tris.

Saturation Transfer. Neither the TOCSY nor the NOESY results will distinguish the specific heme methyl groups, and therefore neither will resolve the ambiguity in assigning the vinyl and propionate resonances. However, since the 2D analysis of MbCO has assigned many heme resonances (Mabbut & Wright, 1985), a saturation-transfer type experiment would connect the deoxy Mb and MbCO signals. Unfortunately a mixture of MbCO and deoxy Mb exhibits no saturation-transfer peaks, but a mixture of oxy Mb and deoxy Mb does. The oxy Mb/deoxy Mb mixture can yield appropriate kinetics data, given the reasonable assumption that MbCO and MbO_2 resonances are similar.

Figure 3A shows a typical 1D 500-MHz proton spectrum of a mixture of deoxy Mb and oxy Mb at 30 °C. The downfield region matches the one from deoxy Mb, which at this temperature separates the $2H_\alpha$ [e] and $4H_\alpha$ vinyl [c] resonances by 1 ppm. Upfield, the characteristic Val E11 γCH_3 of oxy Mb appears precisely at −2.88 ppm, denoted by an arrow. Other upfield resonances correspond to deoxy Mb signals. Panels B, C, and D of Figure 3 display 1D NOE difference spectra upon saturating the prominent deoxy Mb peaks a, d, and h respectively. Irradiating resonance a produces a difference spectrum with a saturation-transfer peak at 2.56 ppm, corresponding to the heme 5-methyl region of oxy Mb, Figure 3B (Mabbut & Wright, 1985). The NOE is about 43%, based on a, as three-proton signal intensity. Imperfect spectral subtraction of the EDTA signals is responsible for the two sharp signals around 3 ppm. Irradiating resonance h produces a saturation-transfer peak at 3.59 ppm, corresponding to the heme 1-, 3-, 8-methyl region of oxy Mb, Figure 3D (Mabbut & Wright, 1985). Irradiating resonance d yields a contrasting result. No saturation peak appears in the oxy Mb heme methyl region. Instead the spillage irradiation on peak c yields a saturation transfer to the oxy Mb $4H\alpha$ signals at 8.47 and 6.38 ppm. Peak e at this temperature is unperturbed by the saturating pulse, which has negligible excitation power 50 Hz away.

2D NOESY maps of a mixture of deoxy and oxy Mb confirm the 1D results and yield additional correlations, Figure 4A. Spectral comparison with the corresponding NOESY map of

Table 1: Assignment of Heme and Heme Pocket Amino Acid Proton Resonances in Horse Heart Deoxymyoglobin in D_2O at 45 °C, pH 7.4

peak label[a]	chemical shift (ppm)[b]	assignment	chemical shift of TOCSY cross peaks (assignment)	chemical shift of NOESY cross peaks (assignment [cross peak no.][c])	reference
a	14.81	5-CH_3		14.08 (6-H_α [161]) 1.58 (6-H_β [18]) 7.92 4.64 2.58 −0.58	La Mar et al. (1993)
b	14.08	6-H_α	6.74 (6-H'_α [1]) 1.58 (6-H_β [2])	14.81 (5-CH_3 [16]) 6.36 (6-H'_β [19])	Yamamoto et al. (1992)
c	13.03	4-H_α	5.10 (4-H_β*trans* [5]) 2.01 (4-H_β*cis* [7])	2.00 [14]	this work
c′	13.03[g]	His 93 H_β			Banci et al. (1993)
d	12.98	Ile 107 γCH_3	9.05 (Ile 107 H_β [4])	7.40 5.31 2.67 2.00 1.66 1.32	this work
e	12.65	2-H_α	3.42 (2-H_β*cis* [6]) −1.84 (2-H_β*trans* [8])		this work
f	12.85	7-H_α	10.91 (7-H'_α [3])		Yamamoto et al. (1992)
g	10.91	7-H'_α	6.44 (7-H_β [9]) 4.26 (7-H'_β [10])	7.30 (8-CH_3)[f]	this work
h	10.78	3-CH_3		9.05 (Ile 107-H_β [17]) 4.98 3.93 2.77 2.00 [14] 1.60 1.32 0.59	La Mar et al. (1993)
i	8.66	His 93 H'_β			Banci et al. (1993)
u	−1.84	2-H_β*trans*	12.65 (2-H_α [8])	7.04 (1-CH_3 [15])[e] 1.61 −0.05 −0.45	this work
v	−2.25	His 97 H_β[d]	−2.87 (His 97 H_β [13]) 2.52 (His 97 H_α [12])		this work
w	−2.87	His 97 H'_β[d]	−2.25 (His 97 H_β [13]) 2.52 (His 97 H_α [11])	−0.58	this work
x	−3.03	not assigned			
y	−4.50	Val 68 γCH_3		0.15 (Val 68 H_β)	Banci et al. (1993)
z	−7.30	Val 68 γCH_3			Yamamoto et al. (1992)

[a] Peak labels are those given in Figure 1. [b] Chemical shifts were determined from TOCSY at 45 °C except where noted. [c] Cross-peak numbers are given in Figure 2. [d] Assignment based on NOE and X-ray structure data. [e] Chemical shift determined from NOESY at 45 °C. [f] NOE cross peak observed from 4.26 ppm resonance (7-H'_β). [g] Peak label is not shown in Figure 1.

Table 2: Summary of Heme Assignments at 45 °C, pH 8.7

assignment	peak label[a]	chemical shift (ppm)
1-CH_3		7.04
3-CH_3	h	10.78
5-CH_3	a	14.81
8-CH_3		7.30
2-H_α-vinyl	e	12.65
2-H_β*cis*-vinyl		3.42
2-H_β*trans*-vinyl	u	−1.84
4-H_α-vinyl	c	13.03
4-H_β*trans*-vinyl		5.10
4-H_β*cis*-vinyl		2.10
6-H_α-propionate	b	14.08
6-H'_α-propionate		6.74
6-H_β-propionate		1.58
6-H'_β-propionate		6.36
7-H_α-propionate	f	12.85
7-H'_α-propionate	g	10.91
7-H_β-propionate		6.44
7-H'_β-propionate		4.26

[a] Peak labels are those given in Figure 1.

deoxymyoglobin, Figure 4B, immediately highlights the saturation-transfer cross peaks, marked with asterisks, Figure 4A. In the downfield region a saturation-transfer cross peak connects b to a resonance at 3.40 ppm. Peak e shows a cross peak to a signal at 8.38 ppm; peak u, to a signal at 5.72 ppm. Upfield, peak y shows a connectivity to a peak at −0.68 ppm. Results are presented in Table 3.

Even though autoxidation produces a small met Mb component during the experiment, the deoxy Mb hyperfine-shifted resonances do not overlap in the downfield region and interfere only slightly in the upfield region (La Mar et al., 1980). The saturation-transfer analysis has focused exclusively on the nonoverlapping signals.

Relaxation. The deoxymyoglobin peaks exhibit characteristic paramagnetic relaxation times, varying from 4 to 62 ms. On the basis of the relationship between molecular distance and the paramagnetic relaxation rate (La Mar et al., 1993), geometric constraints can strengthen the identification of the nucleus associated with each resonance. The results are tabulated in Table 4.

DISCUSSION

Assignment of Heme Groups: (A) Heme Methyl. The ^1H deoxy Mb spectra reveal three dominant signals between 16 and 10 ppm, each with at least three-proton intensity, Figure 1, peaks a, e, and h. Although previous studies have tentatively ascribed them to methyl groups (La Mar et al., 1977, 1978a,b;

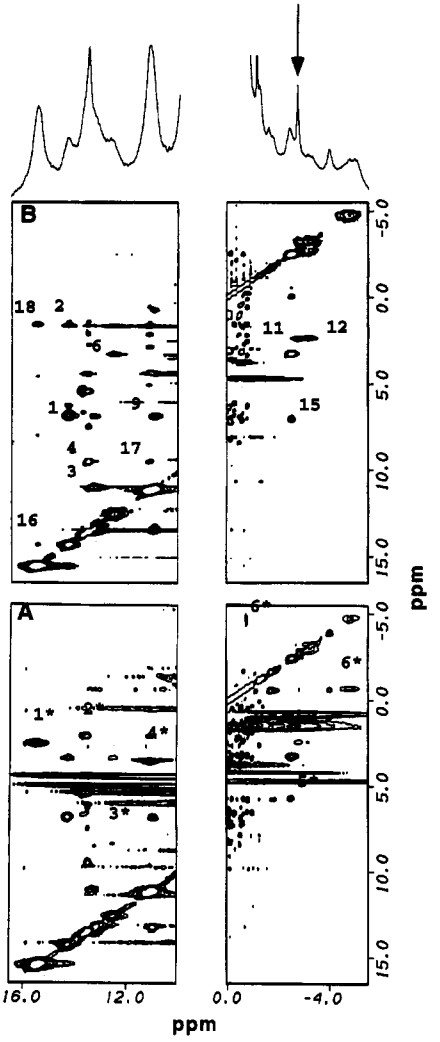

FIGURE 4: (A) Downfield and upfield portions of the 500-MHz 2D NOESY map of a mixture of oxy- and deoxymyoglobin in D_2O, 1 mM EDTA, and 5 mM Tris, pH 8.7, at 30 °C, collected with a 40-ms mixing time. The asterisks identify saturation transfer cross peaks between deoxy- and oxymyoglobin resonances. (B) Downfield and upfield portions of the 400-MHz 2D NOESY map of only deoxymyoglobin in D_2O and 25 mM phosphate buffer, pH 7.4, at 30 °C, collected with a 50-ms mixing time.

Table 3: Summary of Saturation-Transfer Results at 30 °C, pH 8.7

peak label[a]	chemical shift (ppm)	chemical shift of saturation-transfer cross peak (cross-peak labels)[b]	assignment of oxy Mb resonance[c]
a	15.54	2.56 (1*)	5-CH_3
b	14.29	3.40 (2*)	6-H_α-propionate[d]
c	13.55	8.47 (3*)	4-H_α-vinyl
		6.38[e]	4-H_β-vinyl
e	12.55	8.38[e]	2-H_α-vinyl
h	11.17	3.59 (4*)	3-CH_3
u	–2.47	5.72 (5*)	2-H_β*trans*-vinyl
y	–4.73	–0.68 (6*)	Val 68 γCH_3

[a] Peak labels are given in Figure 1. [b] Cross-peak labels are given in Figure 4. [c] Assignments of oxy Mb are given in Mabbutt and Wright (1985). [d] New assignment from this work. [e] Saturation-transfer peak determined from 1D NOE experiment shown in Figure 3.

Yamamoto et al., 1992), the 2D analysis confirms that a and h arise from heme methyl groups. Both signals exhibit no cross peaks in the TOCSY map, Figure 2A. However, in the saturation-transfer experiments, a and h couple to resonances at 2.56 and 3.59 ppm at 30 °C, respectively. These transfer NOE signals in the diamagnetic region correspond directly

Table 4: T_1 Relaxation Times of Hyperfine Shifted Resonances at 45 °C, pH 7.4

peak label[a]	assignment	T_1 relaxation time (ms)
a	1-CH_3	62.8
b	6-H_α-propionate	55.0
c	4-H_α-vinyl	20.0
d	Ile 107 γCH_3	55.2
e	2-H_α-vinyl	30.5
f	7-H_α-propionate	28.8
g	7-H'_α-propionate	49.2
h	3-CH_3	46.1
u	2-H_β*trans*-vinyl	44.4
v	His 97 H_β	65.3
w	His 97 H'_β	44.9
x	not assigned	20.2
y	Val 68 γCH_3	22.4
z	Val 68 γCH_3	<4.0

[a] Peak labels are given in Figure 1.

to the unique 5 (2.56 ppm) and the clustered 1, 3, and 8 (3.59 ppm) heme methyl group positions in oxymyoglobin (Mabbut & Wright, 1985). Peak h, however, has a common NOESY cross peak [14] to the 4H_α vinyl group (vide infra) and indicates that it is then the 3-methyl. A NOESY cross peak [15] between the 2H_β trans (vide infra) at –1.84 ppm and a signal at 7.04 ppm assigns the 1-methyl position at 7.04 ppm. Similarly the connectivity between the 7H'_β at 4.26 ppm and a resonance at 7.30 ppm identifies the 8-methyl position at 7.30 ppm. The heme methyl assignment agrees perfectly with the NMR analysis of protein reconstituted with ^2H or ^{13}C specifically labeled hemes (La Mar et al., 1993; Sankar et al., 1987). The heme methyl order in deoxymyoglobin is then 5, 3, 8, 1 at 14.81, 10.78, 7.30, and 7.04 ppm at 45 °C, respectively.

(B) Heme Vinyl. The 1D saturation-transfer experiments indicate that irradiating peak c produces two signals at 8.47 and 6.38 ppm, corresponding to the oxy Mb 4H_α and 4H_β (Mabbut & Wright, 1985). Moreover peak c shows a consistent common NOE [14] to the 3 heme methyl at 10.78 ppm. Peak c originates then from the 4H_α vinyl group. From the TOCSY map, a consistent heme vinyl spin-coupling pattern appears for both c and e, at 13.03 and 12.65 ppm. Each has also two cross peaks, associated with the respective 4H_β and 2H_β at 5.10 [5], 2.01 [7], 3.42 [6], and –1.84 ppm [8]. Peak e must then correspond to the 2H_α vinyl group. The H_α vinyl assignments are consistent with the ^{13}C-labeling study, which approximates the location of both H_α vinyl groups around 13 ppm in the deoxymyoglobin spectra and the respective signals' temperature dependence (Sankar et al., 1987; La Mar et al., 1978a,b; Yamamoto et al., 1992). The results are tabulated in Tables 1 and 2. An NOE from the 2H_β to the 1 heme methyl as well as a saturation transfer from the deoxy Mb 2H_β signal u at –1.84 ppm [8] to the oxy Mb 2H_β at 5.72 ppm further substantiates the 2H_β vinyl resonance assignment, Table 3.

(C) Heme Propionate. The TOCSY map indicates a spin-coupling pattern consistent with propionate groups, one centered at b and the other at f and g, 14.08, 12.85, and 10.91 ppm, respectively. Peak b couples to signals at 6.74 [1] and 1.58 ppm [2] and shows an NOE cross peak at 6.36 ppm. A strong NOE also connects the heme 5-methyl a to b, suggesting that b then is the 6H_α. Molecular modeling also confirms that the 6H_α proton interacts most closely with the heme 5-methyl. The cross peak at 6.74 ppm [1] shows the strongest intensity, which identifies it as the 6H'_α. The peaks at 6.36 and 1.58 ppm then correspond to the 6H_β. 2D NOESY exchange experiments with the oxy Mb and deoxy Mb mixture

indicate that b is also associated with its diamagnetic partner at 3.40 ppm at 30 °C, Table 3.

Similar reasoning ascribes the peaks at f and g to the $7H_\alpha$. Peak f couples strongly to g. Peak g, moreover, connects to the $7H'_\beta$ at 4.26 ppm, which shows an NOE to the 8 heme methyl at 7.30 ppm. The NOE is consistent with g as the $7H_\alpha$. Peak f is then the $7H'_\alpha$. From g, the cross peaks at 6.44 [9] and 4.26 ppm [10] appear, corresponding to the two $7H_\beta$ signals. The propionate assignments are consistent with the reported observations of Yamamoto et al. (1992) and Banci et al. (1993) and are tabulated in Tables 1 and 2.

(D) Valine 68 (E11). The Val 68 γCH_3 assignment is based on a NOESY exchange cross peak between resonance y and a peak at −0.68 ppm, previously assigned to the oxymyoglobin Val 68 γCH_3 (Mabbut & Wright, 1985). An additional NOE cross peak from y to a peak at 0.15 ppm identifies the deoxymyoglobin Val 68 H_β. T_1 data confirm the assignment and furthermore indicate that the three proton intensity peak z corresponds to the other Val 68 γCH_3. That assignment is based on a a 6-Å calibration distance between the Fe center and the heme methyl as well as the equation

$$T_{1a}/T_{1b} = R^6_{Fe\rightarrow a}/R^6_{Fe\rightarrow b}$$

which relates the relaxation time to the distance R from Fe to the respective nuclei. The relaxation results indicate that z, a methyl group, is within 3.9 Å. Similar reasoning also supports the assignment of y, which is within 5.1 Å. Only Val 68 (E11) has methyl groups within this distance from the heme Fe (Takano, 1977b). The Val γCH_3 assignment is consistent with previous reports (La Mar et al., 1993; Banci et al., 1993; Yamamoto et al., 1992), which assigned the γCH_3 solely on the basis of relaxation data.

(E) Isoleucine 107 (G8). Clearly the three proton intensity peak d does not arise from a heme group. Its common NOESY interaction with the heme 3-methyl localizes the responsible amino acid residue in the heme pocket. Its single TOCSY cross peak at 9.05 ppm [4] supports a CH_3–H_β interaction. Finally its T_1 defines a 6-Å perimeter. Within these experimental constraints, the crystallographic analysis indicates that Ile 107 γCH_3 probably gives rise to signal d. From the Fe center, the Ile γCH_3 is 6.77 Å distant, and the δCH_3, 6.12 Å. Moreover, from the 3 heme methyl, the Ile H_β is 2.33 Å distant, and the γCH_3 is 3.47 Å.

(F) Histidine 93 (F8). Peak c′ at 13.03 ppm is a shoulder resonance that is difficult to resolve. However, 1D transient NOE experiments connect the proximal histidyl NH at 74 ppm at 45 °C with peaks at c′ and i, at 13.03 and 8.66 ppm, respectively (data not shown). These NOE peaks persist, even at short mixing times, ~60 ms, suggesting that they do not arise from spin diffusion. Molecular graphics analysis of the deoxy Mb X-ray crystal structure indicates that the histidyl H_ϵ and the H_β are the closest neighbors, within 2.7 and 3.7 Å of the $N_\delta H$. However, both model compound and protein studies and paramagnetic relaxation considerations indicate that the two broad histidyl H_ϵ signals appear between 40 and 60 ppm (La Mar et al., 1993; Goff & La Mar, 1977). Ascribing the origin of c′ and i to the His 93 H_β and H'_β is consonant with the different NOE intensities, $H_\beta < H'_\beta$, which reflect the different degrees of paramagnetic relaxation due to distance from the heme Fe. Neither the TOCSY nor the NOESY map so far has shown any H_β to H'_β connectivity. Still the assignment favors His 93, consistent with the conclusion from another study (Banci et al., 1993).

(G) Amino Acids in the Heme Pocket. Peaks v and w show a strong TOCSY and NOESY connectivity to each other, which suggests an H_β to H'_β interaction. The T_1 relaxation data restricts the associated amino acid residues to 5.9- and 6.2-Å radii from the Fe center. Based on the geometric and spin system constraints, the molecular graphics analysis of the deoxymyoglobin X-ray crystal structure points to the His 97 FG3 H_β and H'_β as the most likely candidates. A broad one proton intensity peak, x, on the shoulder of w, belongs to another spin system and shows no TOCSY or NOESY cross peaks. The associated proton is approximately 5.2 Å from the Fe and is currently unassigned.

Other NOESY cross peaks appear in the deoxymyoglobin map, most notably from the heme 5-methyl, the Ile 107 γCH_3, and the heme 1-methyl, peaks a, d, and h. Some likely candidates responsible for these cross peaks are His 97, Phe 43, Ile 104, Ile 107, Thr 103, and Ser 108. Additional studies are required to definitively assign these peaks.

Structural Implications: (A) Temperature Dependence. Our ^1H assignment of the deoxymyoglobin heme and the heme pocket signals establishes a basis to probe the iron electronic structure and the heme interaction with the protein environment. In particular these signals' temperature dependent chemical shift is extremely revealing. For a simple, singly populated electronic state, the Curie behavior applies, where $\Delta H_{hyperfine}$ varies linearly with $1/T$ and approaches the $\Delta H_{diamagnetic}$ at infinite temperature, corresponding to the y intercept. For the case when other thermally populated states exist or significant molecular motion is present, both theoretical and experimental studies have demonstrated that a non-Curie behavior will appear and that the resultant chemical shift at infinite temperature will deviate significantly from the diamagnetic position, often expressed as a nonzero intercept in a plot of

$$[(\Delta H/H)_{hyperfine} - (\Delta H/H)_{diamagnetic}] \textit{ vs } 1/T$$

(Jesson, 1973; La Mar & Walker, 1979). Such non-Curie behavior appears in our temperature analysis of the deoxymyoglobin signals and indicates the structural interaction of the vinyl and propionate groups as well as the presence of low-lying but thermally populated electronic states of the heme iron.

(B) Oscillatory Mobility of Vinyl Groups. Many studies have focused on the heme periphery to pinpoint the critical structural interactions that modulate oxygen binding kinetics and the electronic state and have ascribed crucial roles to both the vinyl and propionate groups (Lecomte & La Mar, 1985; La Mar, 1979). One issue is the contrast between the electronic structure in the protein versus the model compound environment mediated by the interaction at the vinyl positions and manifested in the methyl chemical shift spread (La Mar, 1979). With increasingly electronegative substituents at the 4 vinyl position the methyl chemical shift spread of low-spin Fe(III) model compounds gradually mirrors the corresponding signals observed from heme proteins (La Mar, 1979). Although the correlation is not as convincing for high-spin Fe(II) compounds and deoxy heme proteins (Goff & La Mar, 1977; La Mar et al., 1993), it is nevertheless clear that the vinyl groups may play a pivotal role in transmitting protein structural changes to the Fe electronic structure.

Indeed the vinyl groups interact differently with the protein structure in deoxymyoglobin and oxymyoglobin, as expected for heme substituents that relay structural changes. For metcyano and metaquo Mb, models for the ligated state, the 2 vinyl group exhibits greater mobility, on the basis of truncated NOE and temperature dependence analysis (Ramaprasad et al., 1984; La Mar et al., 1980). The temperature dependence

analysis, δ_{ppm} vs T^{-1}, exhibits non-Curie behavior for both the $2H_\alpha$ and the $4H_\alpha$ signals, where the intercepts deviate substantially from their respective diamagnetic positions. Indeed the deviation for $2H_\alpha$ is substantially greater than that for $4H_\alpha$. Such contrasting intercepts indicate that the 2 vinyl group has greater oscillatory mobility than the 4 vinyl group (La Mar et al., 1978b), and the interpretation is consistent with the X-ray crystal structure analysis of the xenon intercalated myoglobin in which the phenylalanine H15 neighboring the 2 vinyl group appears readily displaced (Schoenborn et al., 1965), but the threonine C4 neighboring the 4 vinyl group does not.

In our study of deoxymyoglobin, both the ^1H NMR assignment and the temperature analysis of the 2 and 4 vinyl resonances are now clearly defined. The temperature dependence analysis indicates that the $2H_\alpha$ (e) and $4H_\alpha$ (c) intercepts have shifted substantially from 35 and 15 ppm, as noted in metaquo Mb (La Mar et al., 1980), to 0.17 and 3.3 ppm, which deviate from the respective diamagnetic chemical shifts, 8.35 and 8.42 ppm. Consequently both vinyl groups exhibit decreased oscillatory mobility as myoglobin undergoes the transition from the unligated to the ligated state, but the 2 vinyl group experiences a more pronounced shift in its mobility.

Heme model studies predicate the relationship between temperature dependence and vinyl mobility on the π hyperfine contact interaction, where a coplanar vinyl–heme conformation delocalizes the unpaired spin density into the vinyl π system more efficiently than a perpendicular orientation (La Mar et al., 1978b). In the latter conformation, spin transfer occurs via the σ system or polarization (La Mar, 1973). Specifically, the ratios of the vinyl H_β to the H_α chemical shift, expressed as

$$R_{c,t} = (\Delta H/H)^{H_\beta}_{\text{hyperfine}}/(\Delta H/H)^{H_\alpha}_{\text{hyperfine}}$$

where c,t refers to cis and trans, can give insight into the molecular orientation. For a coplanar conformation, R_c and R_t approximate 1, as in the case for Fe(III) cyano Hb (La Mar et al., 1978). Based on our deoxymyoglobin data, the R_c and R_t values for $2H_\alpha$ and $4H_\alpha$ are 0.5 and 1.7 for the 2 vinyl and 0.9 and 0.3 for the 4 vinyl. Clearly the analysis does not substantiate any coplanar orientation.

A ^{13}C study has given additional insight into the vinyl spin density with its analysis of 2 and 4 vinyl C_α and C_β and associated proton chemical shifts. All ^{13}C resonances are shifted downfield. Whereas the attached H_α resonances are also shifted in the same direction for both groups, the H_β resonances have opposing shifts, with the $4H_\beta$ upfield and the $2H_\beta$ downfield (Sankar et al., 1987). Because contact spin transfer exhibits a sign change in its interaction with carbon and the attached proton, the authors have interpreted their data to reflect a predominant σ transfer, with a slight π spin density on the 4 vinyl β position (Walker & La Mar, 1979). That interpretation is completely consistent with the previous tentative assignment of the 2- and $4H_\beta$ position in the ^1H spectra (Sankar et al., 1987). However, our data indicate that both the 2- and the $4H_\beta$ signals actually experience an upfield shift, Table II, (Mabbut & Wright, 1985) and that a slight π spin density is present at both vinyl positions. Moreover, the upfield shift in the $2H_\beta$ is much greater than that in the $4H_\beta$, suggesting an asymmetric distribution of the π spin density that appears inconsistent with a pure ^5E ground state, where the unpaired spin is shared between the d_{xz} and d_{yz} orbitals.

(C) Conformation of the Propionates. Early molecular dynamics simulations indicate that oxygen can enter the heme via a pathway between Val E11 and His E7, which entails a route through residue 45 (CD3) and the heme 6 propionate (Case & Karplus, 1979). Lecomte and La Mar (1985) have proposed that the electrostatic interactions of the heme 6 propionate, residue 45 (CD3), and Asp 60 (E3) stabilize the "closed door" configuration of His 64 (E7), whose crystallographic rotation suggests its role as a ligand gate (Johnson et al., 1989; Ringe et al., 1984). Their proposal is based on the 30-fold enhancement in the His E7 NH hydrogen exchange kinetics in sperm whale versus dog or horse MbCN, in particular the base-catalyzed protein opening constant, as defined by an EX2 hydrogen exchange mechanism (Woodward & Hilton, 1979). The increased hydrogen exchange rate difference arises purportedly from the additional hydrogen bond between Arg 45 (CD3) and Asp 60 (E3) in sperm whale Mb, whereas such a bond cannot form with Lys 45 (CD3) in horse and dog Mb.

Carver et al. (1991), however, have questioned the role of the heme 6 propionate Lys 45 or Arg 45 salt bridge in regulating ligand entry. Their geminate recombination study of myoglobin with different mutations at position 45 and with a dimethyl ester heme shows only an inhibition of alkyl isocyanide kinetics, and not the overall association constants for O_2, CO, and NO. That observation by Carver et al. (1991) tends to argue against a significant role of the heme 6 propionate in regulating oxygen binding and is consistent with recent molecular dynamic calculations, which indicate that O_2 does not penetrate the heme via the His 64 gateway (Elber & Karplus, 1990).

Although both Lecomte and La Mar (1985) and Carver et al. (1991) have provided invaluable insights, they have observed myoglobin that is not specifically in the deoxygenated state. Determining the role of the heme 6 propionate in controlling ligand entry in the state that binds oxygen is invaluable. Whether the electrostatic interactions of the heme 6 propionate with residue 45 (CD3) and Asp 60 (E3) persist in the unligated state is then a key question. A "mobile" 6 propionate group in deoxymyoglobin would tend to argue against any electrostatic stabilization and would represent a different gating role than a "locked" conformation.

Our deoxymyoglobin temperature analysis reveals that the curves for both the $6H_\alpha$ and the $7H_\alpha$ have intercepts at 12.5 and 19.8 ppm, respectively, which deviate significantly from their diamagnetic positions of 3.40 ppm, as determined in our saturation-transfer experiments. Quite clearly the 7 propionate group exhibits a greater mobility than the 6 propionate group (La Mar et al., 1978b). The different NOEs to the respective methyl groups also are consistent with contrasting mobility, as reported in previous studies of met Mb and MbCN (La Mar et al., 1978a,b, 1980; Ramaprasad et al., 1984; Lecomte & La Mar, 1985). Whereas the $6H_\alpha$ displays a strong NOE to the heme 5-methyl, the 7 propionate group exhibits a weak interaction with the heme 8-methyl. Although our analysis shows contrasting propionate mobility in the unligated state, further work is still required to determine the propionate's role in regulating ligand entry, since structural features by themselves cannot readily yield a kinetics mechanism. But our study establishes the initial set of deoxymyoglobin ^1H NMR assignments and indicates that with saturation transfer, oxygen binding kinetics is obtainable. Consequently, the ^1H NMR strategy can further probe both the deoxymyoglobin structure and function, leading to a potential clarification of the ligand gateway properties in the

heme 6 propionate region.

Electronic Structure: Ground State. The temperature dependence analysis of the deoxymyoglobin signals also yields insight into the electronic structure. Theoretical calculations do not agree on the Fe(II) high-spin electronic ground state, ^5E or $^5B_2$, derived from idealized tetragonal geometry (Eaton et al., 1978; Eicher et al., 1976), but do agree on the existence of several electronic states, closely spaced in energy, which is consistent with Mossbauer quadrupolar splitting and susceptibility data (Huynh et al., 1974; Eicher et al., 1976). La Mar et al. (1993) have argued that the heme rotational disorder in deoxymyoglobin produces a distinctive chemical shift interchange that is consistent with π delocalization in an orbital degenerate ground state with 4-fold symmetry, a ground state derived from ^5E [$(d_{xz})^2 (d_{yz})^1 (d_{xy})^1 (d_{z^2})^1 (d_{x^2-y^2})^1$] or [$(d_{yz})^2 (d_{xz})^1 (d_{xy})^1 (d_{z^2})^1 (d_{x^2-y^2})^1$] rather than $^5B_2$ [$(d_{xy})^2 (d_{xz})^1 (d_{yz})^1 (d_{z^2})^1 (d_{x^2-y^2})^1$]. They have not, however, ruled out a possible contribution from $^5B_2$.

One characteristic feature of different electronic states being thermally populated is hyperfine shifts that deviate from Curie behavior. Although two studies have analyzed the temperature dependence of deoxymyoglobin (Yamamoto et al., 1992; La Mar et al., 1978a), the reported magnitude differs substantially, arising at least in part from the poor resolution in the deoxymyoglobin spectra, which reduces the accuracy in tracking the 1D temperature-sensitive signals over a temperature range. The present study's temperature dependence analysis utilizes both the 1D spectra and the 2D TOCSY maps to improve dramatically the spectral resolution and, as a consequence, overcome some of the uncertainty in determining the Curie behavior. Indeed the results confirm a significant deviation for many deoxymyoglobin signals and support the notion of different populated electronic states, derived from components of ^5E and $^5B_2$. That interpretation is also consistent with the deoxymyoglobin T_1 results, which fall within the range of 20–60 ms, consistent with a short T_{1e} and also with the presence of low-lying states separated by small energy differences.

The most marked deviations from Curie behavior are exhibited in the propionate, Ile 107, and vinyl groups. For both propionate groups, oscillatory mobility can partially explain the large deviation from the diamagnetic position in the intercept values. For the vinyl groups, our data indicate that the intercepts are at 0.17 and 3.2 ppm, shifted upfield from their diamagnetic chemical shift positions at 8.35 and 8.42 ppm. Oscillatory mobility should produce a downfield shift, as observed for metaquo Mb (La Mar et al., 1978b, 1980). Instead, the upfield-shifted intercepts are consistent with a temperature behavior that reflects a dipolar contribution with a T^{-2} dependence, associated with zero field splitting (Jesson, 1973; La Mar & Walker, 1979).

The non-Curie behavior for the peak assigned to Ile 107, peak d, provides further support. Because the contact spin transfer mechanism no longer affects the temperature dependence of the Ile 107 signal, the substantial deviation from Curie behavior must arise from a dipolar interaction, implicating again a significant contribution from the zero field related T^{-2} component.

Yet the model compound study of tetraphenylporphyrin Fe shows only a modest contribution from zero field splitting, as marked either by a deviation from Curie behavior in the heme periphery signals or a substantial axial magnetic anisotropy (Goff & La Mar, 1977). Only in the temperature dependence analysis of the axial 4H imidazole signal does the model compound data hint at such an effect. Our observation then suggests that the deoxymyoglobin environment introduces a rhombic perturbation on the heme and alters significantly the electronic state. The presence of zero field splitting is then consistent with such alteration and indicates different thermally populated electronic states, as La Mar et al. (1993) have suggested in their analysis. However, at present, neither the exact nature of the Ile 107–heme interaction, the magnetic anisotropy, nor the zero field splitting parameter is known with any certainty. Quite clearly the relationship between the electronic structure, the protein structure, and oxygen binding in deoxymyoglobin is neither simple nor direct and warrants further work.

Oxygen Binding Kinetics: Rate Constant. In addition to spectral assignment, the saturation-transfer experiments also can provide insight into the oxygen binding kinetics of Mb. The saturation transfer of the heme 5-methyl spin from the deoxymyoglobin to the oxymyoglobin state produces a 43% change in peak intensity. Peak a's area is used as the normalization constant, Figure 3B. Since the T_1's of the amino acid residues in a diamagnetic protein fluctuate very modestly (Kay et al., 1989), the distinct Val 68 γCH_3 T_1, 101 ms, is a reasonable approximation for the T_1 for the heme 5-methyl in oxymyoglobin.

$$MbO_2 \underset{k_2}{\overset{k_1}{\rightleftharpoons}} Mb + O_2$$

The saturation-transfer experiment yields a pseudo-first-order rate constant (Alger & Shulman, 1983):

$$\frac{I_\infty - I}{I_\infty} = \frac{\lambda}{\lambda + T_1}$$

where I_∞ is the equilibrium signal intensity, I is the peak intensity from the saturation-transfer experiment, λ is $1/k$ for the myoglobin/oxygen reaction, and T_1 is the intrinsic relaxation time. For saturation transfer of the heme 5-methyl from the deoxy to the oxy Mb in a 1:1 mixture, the k_1 is 13 s^{-1}, which is in excellent agreement with previous data (Antonini & Brunori, 1971; Carver et al., 1990). The reverse saturation transfer produced a 25% magnetization change in the heme 5-methyl resonance of deoxy Mb. The selective T_1 is 44.7 ms. Assuming that $[O_2]$ at 50% Mb saturation, $p[O_2]_{50}$, is approximately 1.5 Torr (Wittenberg & Wittenberg, 1989), then k_2 is 27 μM^{-1} s^{-1}, again in good agreement with reported values (Antonini & Brunori, 1971; Carver et al., 1990). The equilibrium constant k_2/k_1 is then 2.0 μM^{-1}.

CONCLUSION

Our study has demonstrated that 2D ^1H NMR can assign the heme and the heme pocket signals of deoxymyoglobin, without recourse to isotopic labeling or mutant protein experiments. The assigned peaks have given insight into the structural perturbations associated with the oxy- and deoxymyoglobin transition. Moreover, the temperature analysis of the hyperfine-shifted peaks supports a ground state that has contributions from both ^5E and $^5B_2$. In turn, saturation-transfer experiments have demonstrated that ^1H NMR can monitor directly the oxygen binding kinetics. Additional studies are underway to utilize the 2D technique to explore fully the deoxymyoglobin structure in order to secure different perspectives on the molecular mechanism regulating the electronic state and oxygen binding.

ACKNOWLEDGMENT

We gratefully acknowledge scientific consultation with Dr. Ulrike Kreutzer.

REFERENCES

Alger, J., & Shulman, R. G. (1983) *Q. Rev. Biophys. 17*, 83–124.
Antonini, E., & Brunori, M. (1971) in *Hemoglobin and Myoglobin in their Reaction with Ligands*, Elsevier North Holland, Amsterdam.
Banci, L., Bertini, I., Marconi, S., & Pierattelli, R. (1993) *Eur. J. Biochem. 215*, 431–437.
Braunschweiler, L., & Ernst, R. R. (1983) *J. Magn. Reson. 53*, 521–529.
Carver, T. E., Rohlfs, R. J., Olson, J. S., Gibson, Q. H., Blackmore, R. S., Springer, B., & Sligar, S. (1990) *J. Biol. Chem. 265*, 20007–20020.
Carver, T. E., Olson, J. S., Smerdon, S. J., Krzywda, S., Wilkinson, A. J., Gibosn, Q. H., Blackmore, R. S., Ropp, J. D., & Sligar, S. G. (1991) *Biochemistry 30*, 4697–4705.
Case, D. A., & Karplus, M. (1979) *J. Mol. Biol. 132*, 343–368.
Dalvit, C., & Wright, P. E. (1987) *J. Mol. Biol. 194*, 313–327.
Eaton, W. A., Hanson, L. K., Stephens, P. J., Stuherland, J. C., & Dunn, J. B. R. (1978) *J. Am. Chem. Soc. 100*, 4991–5003.
Eicher, H., Bade, D., & Parak, F. (1976) *J. Chem. Phys. 64*, 1446–1455.
Elber, R., & Karplus, M. (1990) *J. Am. Chem. Soc.* 112, 9161–9175.
Emerson, S. D., & La Mar, G. N. (1990) *Biochemistry 29*, 1545–1556.
Goff, H., & La Mar, G. N. (1977) *J. Am. Chem. Soc. 99*, 6599–6606.
Ho, C., & Russu, I. (1981) in *Methods in Enzymology* (Antonini, E., Rossi-Bernardi, L., & Chiancone, E., Eds.) Vol. 76, pp 275–312, Academic Press, New York.
Huynh, B. H., Papaefthymiou, G. C., Yen, G. S., Groves, J. L., & Wu, C. S. (1974) *J. Chem. Phys. 61*, 3750–3758.
Jeener, J., Meier, B. H., Bachmann, P., & Ernst, R. R. (1979) *J. Chem. Phys. 71*, 4546–4552.
Jesson, J. P. (1973) in *NMR of Paramagnetic Molecules* (La Mar, G. N., Horrocks, W. DeW., Jr., & Holm, R. H., Eds.) pp 1–51, Academic Press, New York.
Johnson, K. A., Olson, J. S., & Phillips, G. N. (1989) *J. Mol. Biol. 207*, 459–463.
Kay, L. E., Torchia, D., & Bax, A. (1989) *Biochemistry 28*, 8972–8979.
Kreutzer, U., & Jue, T. (1991) *Am. J. Physiol. 30*, H2091–H2097.
Kreutzer, U., Wang, D. S., & Jue, T. (1992) *Proc. Natl. Acad. Sci. U.S.A. 89*, 4731–4733.
La Mar, G. N. (1973) in *NMR of Paramagnetic Molecules* (La Mar, G. N., Horrocks, W. DeW., Jr., & Holm, R. H., Eds.) pp 86–123, Academic Press, New York.
La Mar, G. N. (1979) in *Biological Applications of Magnetic Resonance* (Shulman, R. G., Ed.) pp 305–343, Academic Press, New York.
La Mar, G. N., & Walker, F. A. (1979) in *The Porphyrins* (Dolphin, D., Ed.) Vol. 4B, pp 61–152, Academic Press, New York.
La Mar, G. N., Budd, D. L., & Goff, H. (1977) *Biochem. Biophys. Res. Commun. 77*, 104–110.
La Mar, G. N., Budd, D. L., Sick, H., & Gersonde, K. (1978a) *Biochim. Biophys. Acta 537*, 270–283.
La Mar, G. N., Viscio, D. B., Gersonde, K., & Sick, H. (1978b) *Biochemistry 17*, 361–367.
La Mar, G. N., Budd, D. L., Smith, K. M., & Langry, K. C. (1980) *J. Am. Chem. Soc. 102*, 1822–1827.
La Mar, G. N., Davis, N. L., Johnson, R. D., Smith, W. S., Hauksson, J. B., Budd, D. L., Dalichow, F., Langry, K. C., Morris, I. K., & Smith, K. M. (1993) *J. Am. Chem. Soc. 115*, 3869–3876.
Lecomte, J. T. J., & La Mar, G. N. (1985) *Biochemistry 24*, 7388–7395.
Mabbutt, B. C., & Wright, P. E. (1985) *Biochim. Biophys. Acta 832*, 175–185.
Marion, D., & Wuthrich, K. (1983) *Biochem. Biophys. Res. Commun. 113*, 967–974.
Phillips, S. E. V. (1980) *J. Mol. Biol. 142*, 531–554.
Ramaprasad, S., Johnson, R. D., & La Mar, G. N. (1984) *J. Am. Chem. Soc. 106*, 3632–3635.
Rance, M. (1987) *J. Magn. Reson. 74*, 557–564.
Rance, M., & Cavanagh, J. (1990) *J. Magn. Reson. 87*, 363–371.
Ringe, D., Petsko, G. A., Kerr, D. E., & Ortiz de Montellano, P. R. (1984) *Biochemistry 23*, 2–4.
Sadek, M., Brownlee, R. T. C., Scrofani, S. D. B., & Wedd, A. G. (1993) *J. Magn. Reson. B101*, 309–314.
Sankar, S. S., La Mar, G. N., Smith, K. M., & Fujinari, E. M. (1987) *Biochim. Biophys. Acta 912*, 220–229.
Schoenborn, B. P., Watson, H. C., & Kendrew, J. C. (1965) *Nature 207*, 28–30.
Shulman, R. G., Glarum, S. H., & Karplus, M. (1971) *J. Mol. Biol. 57*, 93–115.
Smith, K. M., Parish, D. W., & Inouye, W. S. (1986) *J. Org. Chem. 51*, 4660–4667.
Takano, T. J. (1977a) *J. Mol. Biol. 110*, 537–568.
Takano, T. J. (1977b) *J. Mol. Biol. 110*, 569–584.
Wittenberg, B. A., & Wittenberg, J. B. (1989) *Annu. Rev. Physiol. 51*, 857–878.
Woodward, C., & Hilton, B. D. (1979) *Annu. Rev. Biophys. Bioeng. 8*, 99–127.
Yamamoto, Y., Iwafune, K., Chujo, R., Inoue, Y., Imai, K., & Suzuki, T. (1992) *J. Biochem. 112*, 414–420.
Yu, L. P., & La Mar, G. N. (1990) *J. Am. Chem. Soc. 112*, 9527–9534.